

**Redox-Active Monolayers in Mesoporous Silicon**

*Simone Ciampi, Bin Guan, Nadim Darwish, Peter J. Reece, J. Justin Gooding\**

*Continuing from Ref. [18]:* The mechanism(s) of PSi formation in HF is still debated.<sup>1</sup> A definitive model to account for the difference in dissolution rates at pore tips and pore walls, in particular for mesoporous p-type PSi, is still lacking. There is, however, a general consensus that for p-type material transfer of electron holes leading to PSi formation is likely to take place under moderate depletion of the majority charge carriers<sup>2</sup> (*i.e.* biasing cathodic of the flat-band potential,  $E_{FB}$ ),<sup>3,4</sup> and local thinning of the depleted SCL at the pore tips may here facilitate the carrier transfer and lead to pores formation.<sup>5</sup>

During the porous etching the dissolution reaction can be considered to occur at an array of electrodes, the pore tips, while the majority of the PSi matrix remains electrochemically inactive. The anodization in HF requires first two electron holes to convert Si-H to Si-OH terminations, which are either chemically replaced by highly polar Si-F bonds, or further oxidized by electron holes to SiO<sub>2</sub> (*i.e.* electropolishing).<sup>6</sup> Competition between the kinetics of the chemical dissolution of the Si-F surface and the rate of silica (SiO<sub>2</sub>) formation determines whether PSi forms or whether electropolishing occurs.<sup>7</sup>

While formation of micropores is commonly understood as due to quantum size effects,<sup>8</sup> the formation of larger pores is perhaps dominated by the electric field of the SCL. The various models have been reviewed by Chazalviel and co-workers.<sup>1a</sup> For the case of macropores, Lehmann has proposed a model in which there is diffusion current toward the surface. However, since the electrode is under slight reverse bias, however, a field current in the opposite direction exists. When positive potentials are applied, their effects are negligible on the diffusion current but sizeable on the field current. The field current decreases to the extent where the dissolution reaction is now governed by the diffusion current. Due to geometrical factors silicon dissolution is indeed much faster at the pores tips and a porous structure forms. For highly-doped p-type substrates, as those used in this study, mesoporous formation is however likely due to tunneling effects.<sup>5</sup> Similar observations under moderate depletion are reported in HF-free electrolytes,

where, in a situation that closely recalls PSi formation, electrochemical passivation of pore walls against cathodic reactions limits current flows to the pore tips only.<sup>9</sup>

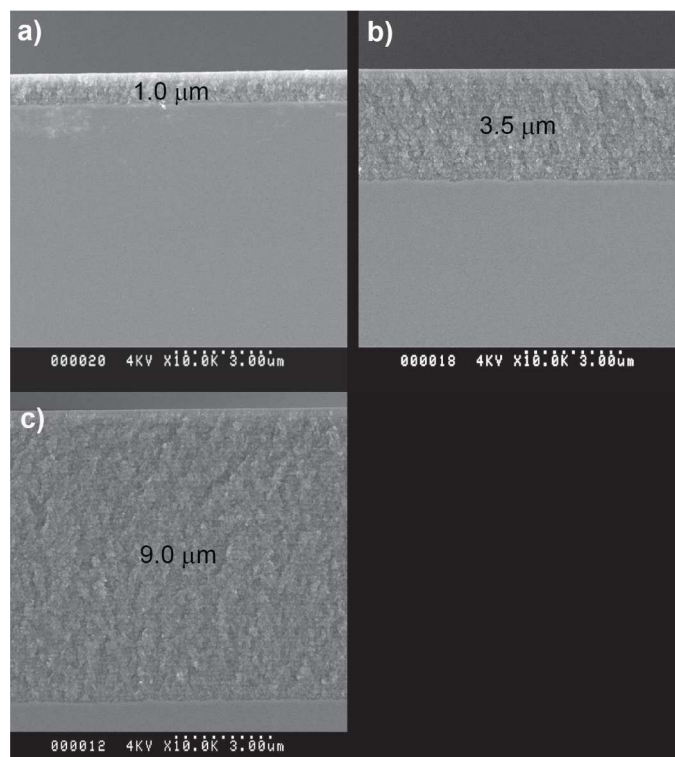


**Figure S1.** Cross-section SEM micrographs for as-prepared  $(\text{Si}\square\text{H}_x)$   $\text{p}^+$  PSi samples. (a) (LH) 6, (b) (LH) 20, and (c) (LH) 60.

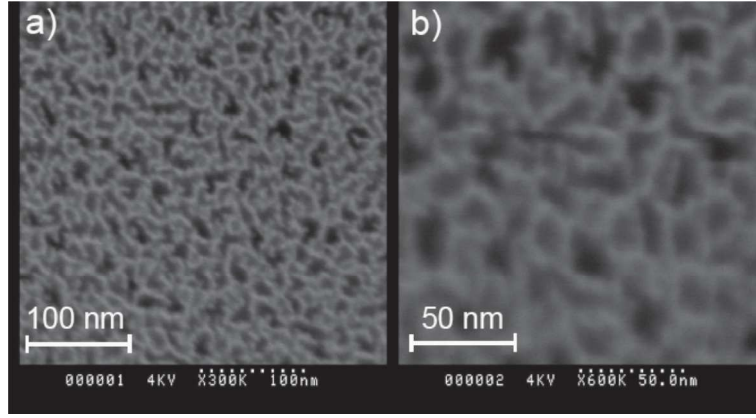


**Figure S2.** Top view scanning electron micrographs for  $p^+$  PSi samples (0.07 ohm cm,  $N_A = 4.8 \times 10^{17} \text{ cm}^{-3}$ ) at a magnification of (a)  $\times 300$  K and (b)  $\times 600$  K.

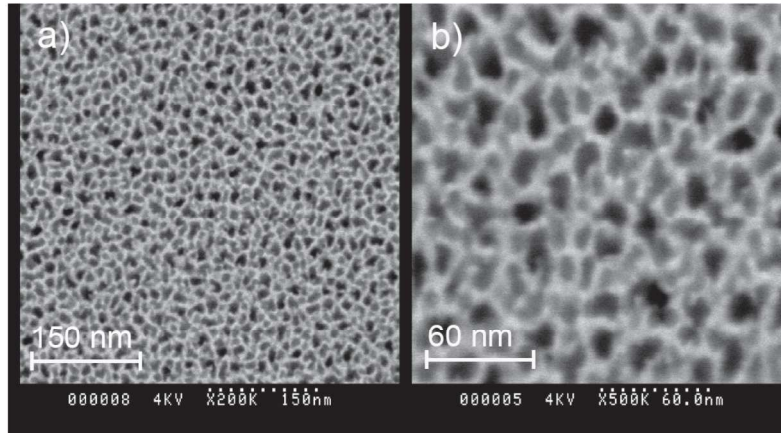


**Figure S3.** Top view scanning electron micrographs for  $p^{++}$  PSi samples (0.0015 ohm cm,  $N_A = 7.7 \times 10^{19} \text{ cm}^{-3}$ ) at a magnification of (a)  $\times 200$  K and (b)  $\times 500$  K.

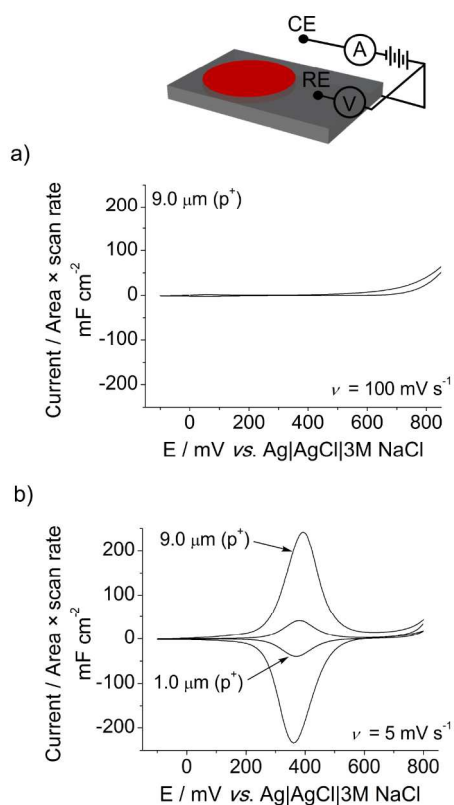


**Figure S4.** Cyclic voltammetry of **SAM-1** and **SAM-2** PSi samples in 1.0 M HClO<sub>4</sub>. (a) Voltammograms of **SAM-1** samples ( $p^+/9.0 \mu\text{m}$ ) in contact with a solution of pure electrolyte in the absence of immobilized or dissolved redox species. (b) Oxidation and reduction waves from tethered Fc units of **SAM-2** samples ( $p^+/1.0$  and  $9.0 \mu\text{m}$ ). Currents values are normalized to the electrode geometric area ( $24.6 \text{ mm}^2$ ) and scan rate ( $\nu$ ).

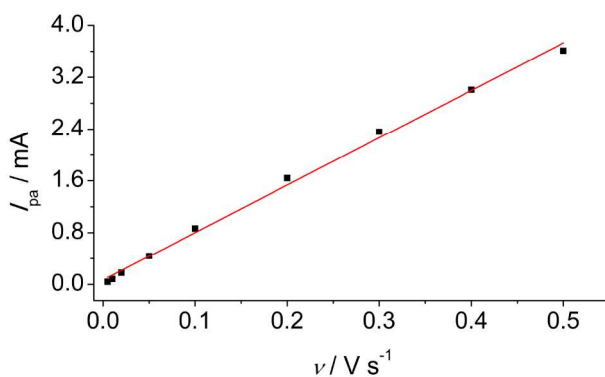


**Figure S5.** Anodic peak current ( $I_{pa}$ ) as a function of scan rate,  $\nu$ , for **SAM-2** samples ( $p^+$ /1.0  $\mu\text{m}$  thick PSi layer). Electrolyte was 1.0M  $\text{HClO}_4$ .

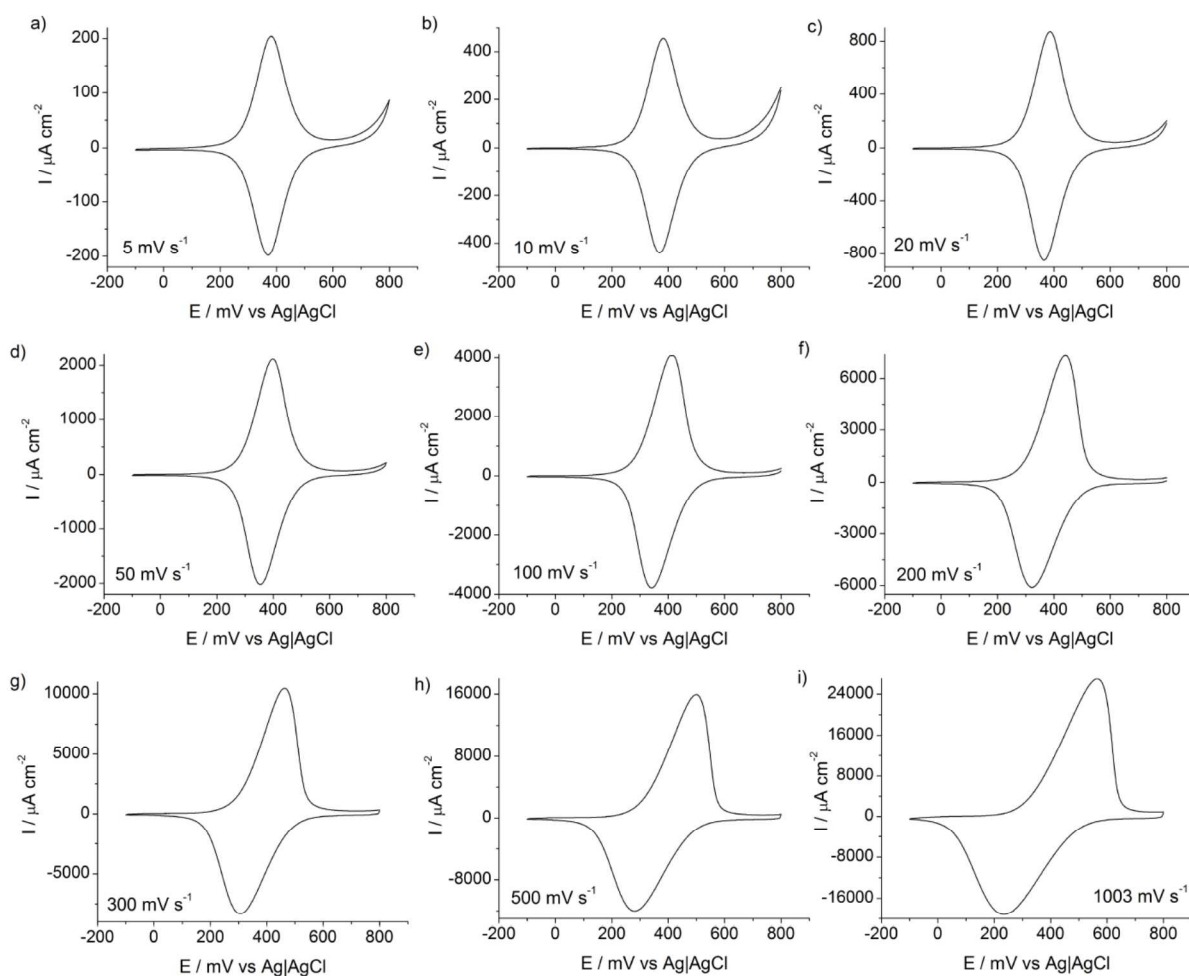


**Figure S6.** Cyclic voltammograms for  $p^+$ , 1.0  $\mu\text{m}$  thick PSi electrodes (**SAM-2**). Scan rates values are indicated in each plot, and current values are normalized for the electrode geometric area (24.6  $\text{mm}^2$ ). Electrolyte was 1.0 M  $\text{HClO}_4$ .

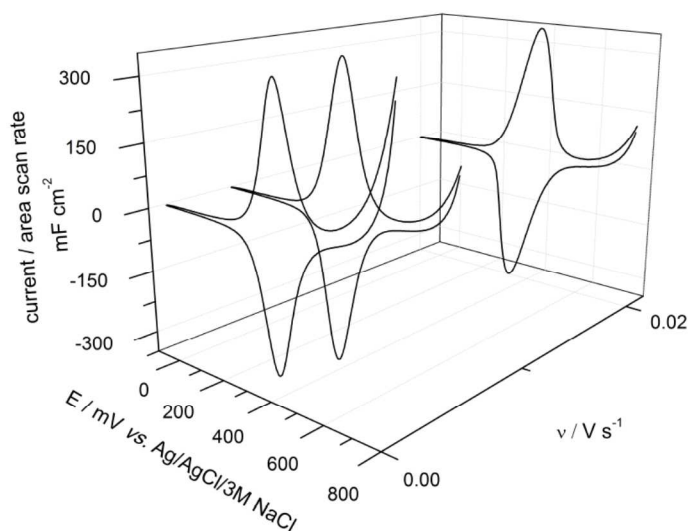


**Figure S7.** Cyclic voltammograms (normalized to geometric area and scan rate) as a function of scan rate for **SAM-2** samples ( $p^+/9.0 \mu\text{m}$  thick PSi layer).

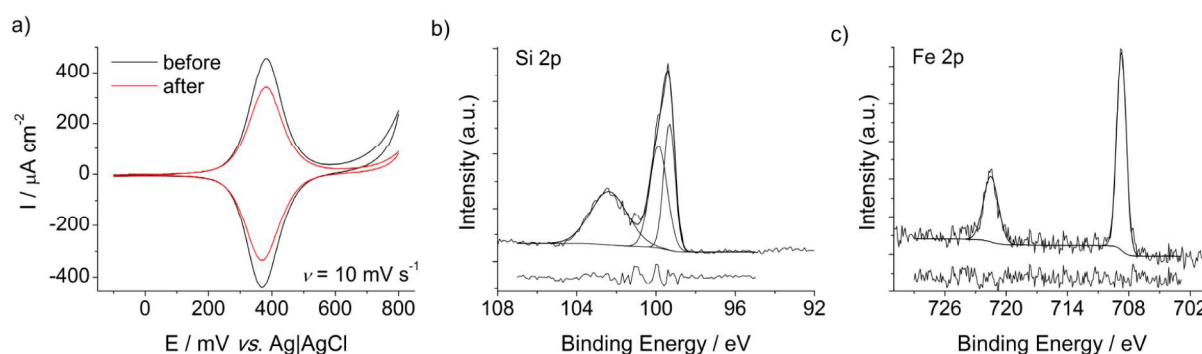


**Figure S8.** (a) Representative cyclic voltammograms ( $\nu = 10 \text{ mV s}^{-1}$ ) of **SAM-2** PSi samples ( $p^+/1.0 \mu\text{m}$ ) before (—) and upon (—) prolonged cyclic voltammetry analysis ( $\sim 100$  CV cycles) in  $1.0 \text{ M HClO}_4$  electrolytes. The measured ferrocene coverage, normalized for the electrode geometric electrode area,  $\Gamma$ , decreased to  $4.7 \times 10^{-8} \text{ mol cm}^{-2}$  ( $4.5 \text{ mC cm}^{-2}$ ) from  $5.7 \times 10^{-8} \text{ mol cm}^{-2}$  ( $5.5 \text{ mC cm}^{-2}$ ) and  $\Delta E_{\text{fwhm}}$  increased only marginally to 119 from 113 mV. Peak positions were unaltered. (b-c) High-resolution XPS scans of the Si 2p and Fe 2p region for the PSi electrode after the extensive CV analysis. The absence of Fe(III) 2p emissions, generally associated to ferrocenium ion when non-negligible SiOx species appears needs further investigation.

## References

- (1) a) Chazalviel, J. N.; Wehrspohn, R. B.; Ozanam, F. *Mater. Sci. Eng., B* **2000**, 69–70, 1; b) Zhang, X. G. *J. Electrochem. Soc.* **2004**, 151, C69.
- (2) Despite the exact electronic band configuration during PSi formation being not yet totally clear, SiO<sub>2</sub> formation and electropolishing would then seem to occur, in HF-based electrolytes, under hole accumulation (i.e. anodic of EFB) and over the entire PSi matrix.
- (3) Ottow, S.; Popkirov, G. S.; Föll, H. *J. Electroanal. Chem.* **1998**, 455, 29.
- (4) a) Gaspard, F.; Bsiesy, A.; Ligeon, M.; Muller, F.; Herino, R. *J. Electrochem. Soc.* **1989**, 136, 3043; b) Wijesinghe, T. L. S. L.; Li, S. Q.; Blackwood, D. J. *J. Phys. Chem. C* **2007**, 112, 303.
- (5) Lehmann, V.; Stengl, R.; Luigart, A. *Mater. Sci. Eng., B* **2000**, 69-70, 11.
- (6) a) Allongue, P.; Kieling, V.; Gerischer, H. *Electrochim. Acta* **1995**, 40, 1353; b) Blackwood, D. J.; Zhang, Y. *Electrochim. Acta* **2003**, 48, 623.
- (7) Memming, R.; Schwandt, G. *Surf. Sci.* **1966**, 4, 109.
- (8) Lehmann, V.; Gosele, U. *Appl. Phys. Lett.* **1991**, 58, 859.
- (9) Bsiesy, A.; Gelloz, B.; Gaspard, F.; Muller, F. *Appl. Phys. Lett.* **1996**, 79, 2513.